Tunable, High-Power, Subpicosecond Blue-Green Dye Laser System with a Two-Stage Dye Amplifier

Tracy E. Sharp, *Student Member, IEEE,* C. Brent Dane, Duane Barber, Frank K. Tittel, *Fellow, IEEE,* Peter J. Wisoff, *Member, IEEE,* and Gabor Szabó

Abstract—**A two-stage dye amplifier design has been developed to amplify tunable, blue-green, subpicosecond dye laser pulses which are generated from a hybrid synchronously mode-locked dye oscillator directly (800 fs) or shorter to 200 fs by a fiber compressor stage. This system has achieved single pulse energies of 2 mJ, with an amplified spontaneous emission content of less than 0.1%. Using 40 mJ of the third-harmonic output of an Nd:YAG regenerative amplifier to pump the dye amplifier system, these pulse energies represent an energy extraction efficiency of ~5%. The tunability, stability, and spatial and temporal quality of the output pulses from the system have also been characterized.**

Introduction

RECENTLY the extension of the spectral range of subpicosecond laser sources to the blue-green has been accomplished using colliding pulse mode-locked dye lasers [1], synchronously pumped dye lasers [2], distributed feedback dye lasers [3], and white light continuum filtering [4], [5]. The amplification of blue-green subpicosecond laser pulses to the millijoule level is difficult because of the relatively few suitable saturable absorbers available to reduce the amplified spontaneous emission (ASE) between amplifier stages. This limits the suitability of the three-stage, 1 mJ amplifier design previously used with rhodamine dyes [6]. Regenerative amplifiers producing short pump pulses have been used with three-stage amplifier designs, which often still incorporate saturable absorbers, to amplify both rhodamine [7] and styryl dyes [8], but have not been applied to the blue-green region of the spectrum. This paper presents a new two-stage amplifier system pumped by the third harmonic of the output from an Nd:YAG regenerative amplifier. This system can produce tunable 2 mJ, 800 fs single pulses in the blue-green region of the spectrum with an ASE content of less than 0.1% without the use of saturable absorbers in the amplifier stages. With the addition of a fiber compressor stage, the pulse duration was shortened to 200 fs with only a 20% decrease in the output energy, although this reduced the tuning range by half. This system has recently been used to characterize a new femtosecond XeF($C \rightarrow A$) excimer laser amplifier, resulting in output energy densities as high as 170 mJ/cm^2 [9].

Manuscript received September 28, 1990; revised January 14, 1991.

This work was supported by the U.S. Air Force Office of Scientific Research, the U.S. Office of Naval Research (DARPA University Research Initiative), and the Welch Foundation.

T. E. Sharp, C. B. Dane, D. Barber, F. K. Tittel, and P. J. Wisoff are with the Department of Electrical and Computer Engineering and the Rice Quantum Institute, Rice University, Houston, TX 77251.

G. Szabó is with the Department of Optics and Quantum Electronics, JATE University, H-6720 Szeged, Dom ter 9, Hungary.

IEEE Log Number 91446430

System Design

The laser system is schematically depicted in Fig. 1. A hybridly mode-locked dye laser pumped by the third harmonic of a CW mode-locked Nd:YAG laser (Coherent Antares 76-s) produced 800 fs laser pulses tunable in the blue-green spectral region. The system originally used a KTP crystal for frequency doubling, providing 4 W of power in the second harmonic, and a BBO crystal for third-harmonic generation by sum frequency mixing, providing 1 W of power at 355 nm; however, increased system performance was achieved by replacing both crystals with LBO. The second-harmonic generation efficiency was improved by replacing the KTP crystal with a 12 mm long LBO crystal cut for type I noncritical phase matching. The higher damage threshold of the LBO and the noncritical phase matching allowed the use of tighter focusing, thus increasing the power at 532 nm up to 7.5 W [10]. The high angular sensitivity of the BBO for third-harmonic generation resulted in a noncircular beam shape that required a cylindrical compensating lens in order for the 355 nm pump beam to match the dye laser mode. The BBO in the third-harmonic generator was replaced by a 10 mm long LBO cut for type II phase matching, producing 1.3 W at 355 nm. Although LBO crystals had been previously used for third-harmonic generation with Q-switched Nd:YAG lasers [11], to our knowledge, this was the first application of this new nonlinear material for third-harmonic generation with CW mode-locked Nd:YAG lasers. The use of LBO for the generation of the third-harmonic pump beam was found to be crucial for stable operation of the dye laser because of the nearly circular spatial profile of the UV beam, as well as improved long-term stability of the third-harmonic output power above the 800 mW pump power threshold.

The dye oscillator was a modified Coherent 702 hybrid

0018-9197/91/0500-1221$01.00 © 1991 IEEE

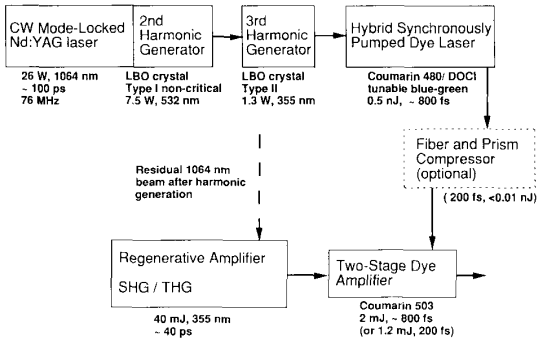

Fig. 1. Schematic diagram of the subpicosecond blue-green dye laser system.

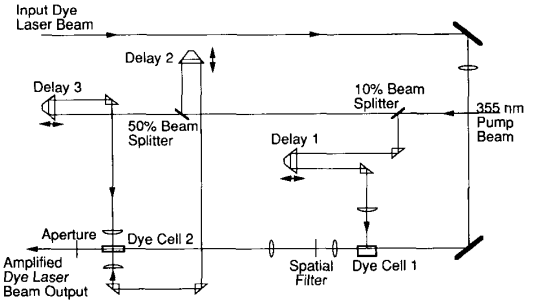

Fig. 2. Experimental layout of the two-stage dye amplifier.

synchronously mode-locked dye laser (coumarin 480/DOCI). A high-resolution differential micrometer was installed on the dye laser for cavity length adjustments since the cavity length tolerance with third-harmonic pumping was found to be more sensitive than that with second-harmonic pumping, presumably due in part to the lower gain of the blue dyes and the shorter pulse duration of the third-harmonic pump pulse. The output coupler was also placed in a dual-axis gimbal mount to decouple angular adjustments from the cavity length.

The vertically polarized dye oscillator output beam was then injected into a two-stage amplifier chain designed to be pumped by the picosecond pulses from a regenerative amplifier. The regenerative amplifier shown in Fig. 1 was configured with a closed-cavity amplifier and one external Nd:YAG amplifier (Continuum Corporation RGA-69). This regenerative amplifier, seeded by the residual 1064 nm radiation from third-harmonic generator, could produce 250 mJ, 1064 nm laser pulses at a 6 Hz repetition rate. The 1064 nm output was then converted to the third harmonic, resulting in 40 mJ, ~40 ps pulses at 355 nm. After using a wave plate to rotate the 355 nm pump beam polarization to a vertical orientation to match the polarization of the dye laser beam, the 355 nm pulses were used to pump the two-stage dye amplifier system shown in Fig. 2. The dye amplifier consisted of two transversely pumped dye cells. The first dye cell was pumped by 10% of the pump beam, and the second dye cell was pumped symmetrically with two transverse pump beams. The three delay prisms were used to adjust the synchronism between the pump beam and the injected dye laser beam. The injected dye laser beam at the first dye cell had a beam radius of 0.2 mm with an average power of ~20 mW, corresponding to an injected energy density of 2×10^{-7} J/cm^2. The output of the first dye cell was spatially filtered using the telescope and aperture arrangement shown in Fig. 2 to reduce the ASE and to increase the dye laser beam diameter to ~2 mm for injection into the second dye cell. The second dye cell had a 2 mm wide channel through which the dye flowed. The presence of the narrow channel allowed symmetrical transverse pumping to achieve a relatively uniform energy deposition in the dye. The final amplifier output was then passed through an aperture to remove any off-axis ASE.

The optional fiber and prism compressor shown in Fig. 1 could be added to the system to compress the dye pulses, as described later.

System Performance

A tuning curve for the dye oscillator operating with coumarin 480 dye and DOCI as the saturable absorber is shown in Fig. 3. At a 76 MHz mode-locking frequency and an average third-harmonic pump power of 1 W, the peak energy per dye oscillator pulse was approximately 0.8 nJ at 480 nm and 0.4 nJ at 500 nm. The amplitude stability of the output of the dye oscillator was very good for a few hundred pulses; however, oscillations in the pulse amplitude occurred with two different frequencies, resulting in ~10% peak-to-peak noise. The faster of the two oscillations (~10 μs period) was also observed in the 355 nm pump beam, and corresponds to the frequency of the switching circuit for the power supply for the Antares lamps. The slower oscillation (~40 μs period) was not observed in the pump beam, and may come from mechanical instabilities in the dye jets. This oscillation also corresponded to a spectral shift in the output of the dye laser which is believed to result from the accumulation of self-phase modulation in the dye laser. The dye oscillator pulse length was measured using a multishot background-free autocorrelator (Inrad 5-14A) with a 0.5 mm thick BBO crystal. A typical intensity autocorrelation is shown in Fig. 4. The FWHM is about 1.2 ps, corresponding to a pulse length of ~780 fs (FWHM) for a sech^2 pulse shape.

Tuning curves for the two-stage dye amplifier system are shown in Fig. 5 for both coumarin 480 and coumarin 503. Two dyes were needed in the amplifier to cover the entire wavelength range of the dye oscillator operating with coumarin 480/DOCI because of the spectral shift of the dyes in the different solvents (ethylene glycol and benzyl alcohol in the oscillator, methanol in the amplifiers). The pulse energy was measured with a pyroelectric joulemeter (Molectron J25LP) attached to a peak reading display (Molectron JD 1000) that used an internal trigger and auto baseline correction feature to discriminate between the amplified pulses and the unamplified 76 MHz

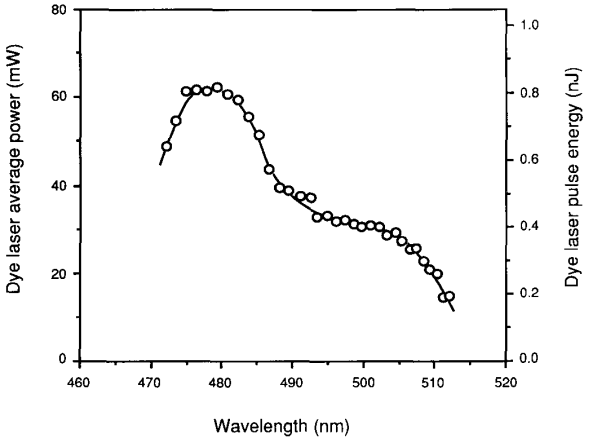

Fig. 3. Tuning curve for the dye oscillator with coumarin 480 as the gain medium and DOCI as the saturable absorber.

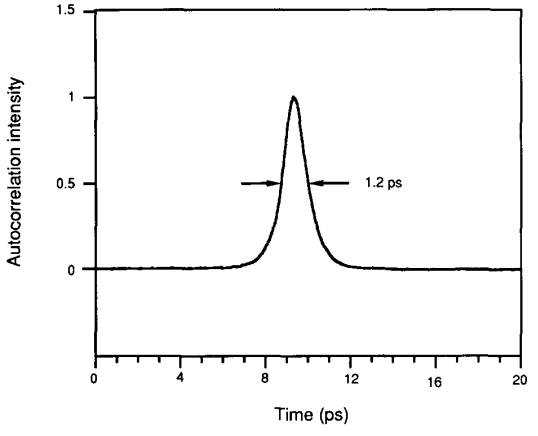

Fig. 4. Autocorrelation trace of the dye oscillator output. The data were measured with a multishot, background-free autocorrelator with a 0.5 mm BBO crystal. The 1.2 ps (FWHM) autocorrelation width corresponds to a pulse length of 780 ps, assuming a sech^2 pulse shape.

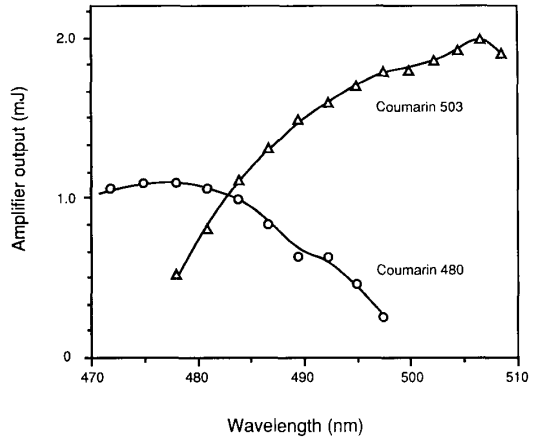

Fig. 5. Tuning curves for the dye amplifier with coumarin 480 and coumarin 503 as the amplifier dye. For both curves, the oscillator was operating with the coumarin 480/DOCI setup.

pulses. The typical energy throughput for the unamplified pulses was ~ 250 pJ/pulse. The peak pulse energy obtained from the amplifiers was ~ 2 mJ, corresponding to an efficiency of 5% using 40 mJ of 355 nm pump energy. This represents a large efficiency for subpicosecond amplification, particularly in the relatively low-gain coumarin dyes. To achieve this output efficiency, both amplifier cells were operated at roughly the same saturation levels, with an output of 25 μJ from the first cell representing an output energy density of ~ 20 mJ/cm^2 which, after beam expansion and spatial filtering, resulted in an input energy density of ~ 0.25 mJ/cm^2 to the second dye cell. It should also be noted that, because of the relatively high pump energy, the amplified pulse energy decreased fairly rapidly, with the dyes needing to be changed after about three days of operation for the best performance of the amplifier chain.

Figs. 6 and 7 show an autocorrelation trace of an amplified dye laser pulse taken with a phase-sensitive single-shot autocorrelator [12]. The line in Fig. 6 indicates a fit to the data assuming a sech^2 pulse shape, while the line in Fig. 7 represents the fit assuming an asymmetric exponential pulse with a rise/fall ratio of 1 : 5. It is clear that the assumed asymmetric pulse shape gives much better agreement than the sech^2 pulse shape, especially in the wings where the calculated sech^2 curve decays much faster than the measured curve. Because the investigated pulses are amplified by a saturated amplifier chain, it is not surprising that the sech^2 pulse shape (or any other symmetric pulse shape) does not give a good fit since one would expect that the pulses are asymmetric (although not necessarily broadened) after passing through the amplifier. Moreover, the main difference between the sech^2 pulse and the asymmetric exponential pulse is the asymmetry since the sech^2 pulse also decays as $\exp(-t)$. The corresponding asymmetric fit to the data represents a pulse duration of 800 fs (FWHM). The single-shot autocorrelation measurement of the amplified dye pulse provided a sensitive diagnostic for adjusting the dye oscillator cavity length since satellite pulses in the amplifier output could be observed with the single-shot autocorrelator when the dye oscillator cavity length was detuned.

The ASE content of the amplifier output was measured by spectrally separating the ASE from the dye laser pulse with an SF-14 prism. The expanded spectrum filled the aperture of a vacuum photodiode. The injected dye laser beam was blocked prior to the photodiode, and the relative differences in signal intensity were measured with the photodiode. Using this method, the ASE was found to be less than 0.1% of the output energy.

The sensitivity of the output energy of the amplifier to the synchronism of the pump pulse and the injected dye laser pulse is shown in Fig. 8. The points represent the output energy of the first dye stage, measured while adjusting the first delay prism in Fig. 2 to change the timing between the pump pulses and the injected dye laser pulses at the first dye cell. As indicated in Fig. 8, the timing was sensitive to within 10 ps of delay to achieve optimal per-

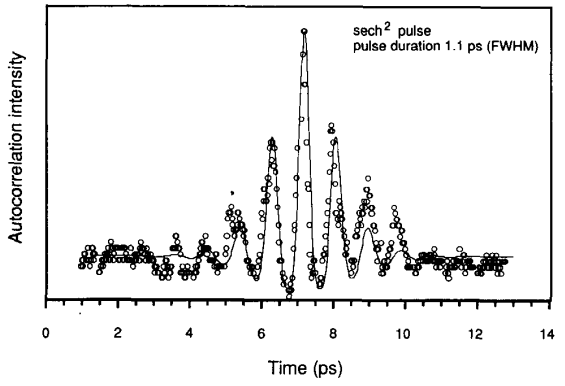

Fig. 6. Autocorrelation trace of the dye amplifier output measured with a phase-sensitive single-shot autocorrelator [12]. The line indicates the calculated fit to the data assuming a sech^2 pulse with a corresponding pulsewidth of 1.1 ps (FWHM). The calculated fit differs noticeably from the data in the wings of the pulse where it decays much faster than the data.

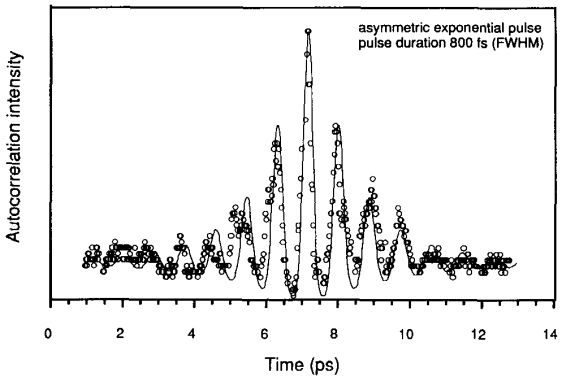

Fig. 7. Autocorrelation trace of the dye amplifier output measured with a phase-sensitive single-shot autocorrelator [12]. The line indicates a calculated fit to the data assuming an asymmetric exponential (1 : 5 rise/fall ratio) pulse with a corresponding pulsewidth of 800 fs (FWHM). This asymmetric pulse is considered to be a better approximation to the pulse shape because of the amplification by a saturated amplifier chain. The agreement between the calculated fit and the data is much better here than in Fig. 6, which is most noticeable in the wings of the pulse.

formance. The solid line in Fig. 8 shows the temporal duration of a pump pulse from the regenerative amplifier measured by a 2 ps resolution streak camera (Hammamatsu-C1587). The overlap of the temporal shape of the pump pulse and the timing sensitivity of the amplifier suggests that the sensitivity is directly related to the very short duration of the pump pulse (~ 40 ps) and that, because of the presence of the ASE, the inversion decays with the pump pulse and not with the spontaneous lifetime of the dye.

Because the dye laser system was designed as an injection source for the XeF($C \rightarrow A$) amplifier [9], it was necessary to have a smooth injection beam profile at the excimer amplifier. The symmetric transverse pumping of the second dye cell allowed the generation of a uniform pump density in the gain medium, resulting in a uniform beam

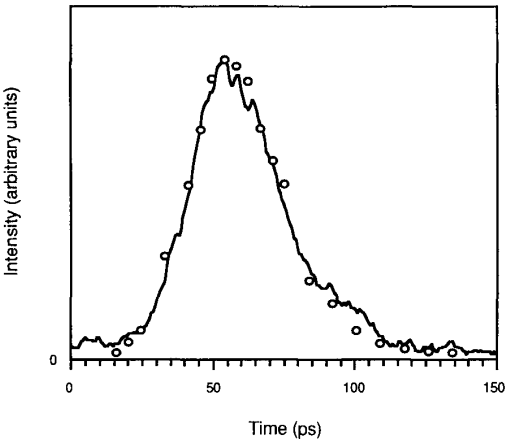

Fig. 8. Sensitivity of the output energy of the dye amplifiers to the synchronism of the pump pulse and the dye laser pulse. Points represent the output energy of the first dye stage, measured while adjusting the first delay prism in Fig. 2 to change the timing between the pump pulses and the injected dye laser pulses at the first dye cell. The solid line shows the temporal shape of the pump pulse from the regenerative amplifier measured with a streak camera. The intensity scales are normalized.

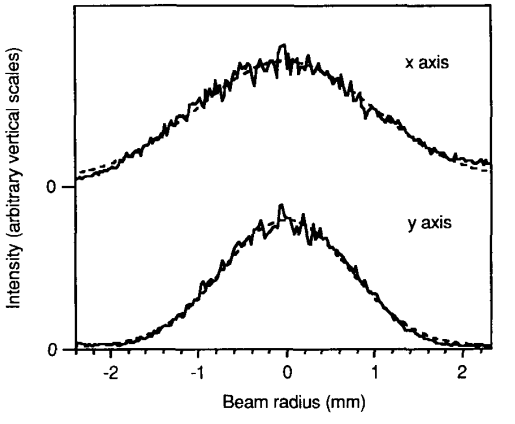

Fig. 9. Spatial profiles of an amplified dye laser pulse in the x and y directions. The profiles were taken in the far field of the beam (13.4 m from the last dye cell). The dotted curves show Gaussian fits to the profiles, indicating a near Gaussian beam profile from the amplifier. The divergence of the beam was 0.25 mrad.

profile in the far field. Fig. 9 shows the spatial profile of the output dye laser pulses ($\lambda = 490$ nm) in the far field (13.4 m from the second amplifier dye cell) along the x and y axes obtained with a CCD beam profiling system. The near Gaussian far field beam profile is indicated by the Gaussian fit shown in Fig. 9. The ratio of the beam radii in the x and y directions was approximately 1 : 1.5 for this transverse method of pumping. The intensity distribution very close to the dye amplifier (< 1 m) was not Gaussian, but resembled a flat-top distribution. The divergence of the beam was 0.25 mrad, indicating that the beam is about 3.5 times the diffraction limit for a Gaussian beam, assuming a spot size of 2 mm diameter (the size of the beam in the second dye cell).

Pulse Compression

As shown in Fig. 1, an optional fiber and prism compressor could be added to the system prior to the dye amplifier to produce ~200 fs pulses. This addition, however, restricted the system to operation at wavelengths above 488 nm, the cutoff wavelength for single-mode operation of the fiber, thereby reducing the tunability of the system. The experimental setup for compression consisted of a 92.7 cm length of a polarization-preserving, single-mode fiber for the blue–green spectral region (Newport F-SPA), designed for single-mode operation between 488 and 514 nm, and two 60° SF-14 prisms used as a double-pass prism compressor. Losses through the fiber and prism pair were ~80%, resulting mainly from the low coupling efficiency into the 1.5 μm core diameter fiber (the prisms were used near Brewster's angle for high transmission).

The optimum fiber length and achievable pulse compression for this setup were calculated from a theoretical analysis described by Tomlinson *et al.* [13]. Accordingly, the normalized soliton length is defined to be

$$z_0 = 0.322 \frac{\pi^2 c^2 \tau_0^2}{|D(\lambda)|\lambda} \tag{1}$$

and the normalized peak amplitude is

$$A = \sqrt{P/P_1} \tag{2}$$

where

$$P_1 = \frac{nc\lambda A_{\text{eff}}}{16\pi z_0 n_2} \times 10^{-7}\ \text{W} \tag{3}$$

τ_0 is the intensity FWHM of the input pulse, $D(\lambda)$ is the group velocity dispersion in dimensionless units, n is the refractive index of the core material, n_2 is its nonlinear coefficient in electrostatic units (1.1×10^{-3} esu for silica), c is the velocity of light in centimeters per second, λ is the vacuum wavelength in centimeters, P is the peak power of the input pulse, and A_{eff} is an effective core area (which is approximately equal to the core area). For our fiber, $n = 1.467$, and $A_{\text{eff}} = 1.77 \times 10^{-8}$ cm^2. The dispersion of the fiber was determined from previous work to be 0.666 ps/nm · m [14], giving $D(\lambda) = 0.0979$ at $\lambda = 490$ nm. For an input pulse width of ~800 ps, the soliton period z_0 is 3.78 m, and P_1 for our pulses is 1.99 W, giving a normalized pulse amplitude A of 6.43. The optimum fiber length for compression and the compression ratio are given by [13]

$$\frac{z_{\text{opt}}}{z_0} \approx \frac{1.6}{A} \tag{4}$$

and

$$\frac{\tau_0}{\tau} \approx 0.63A. \tag{5}$$

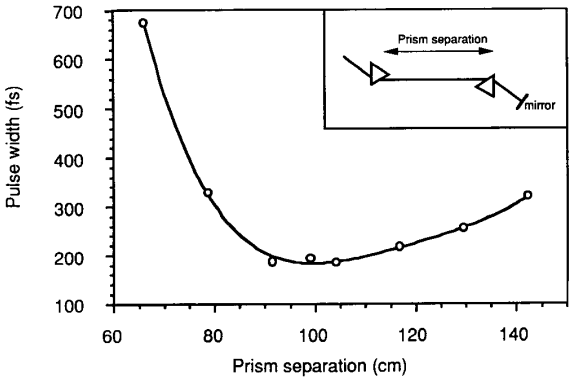

Fig. 10. Pulse duration after the fiber and prism compressor as a function of the compressor prism separation. The pulse durations were measured with a multishot autocorrelator. Each data point is the average of the pulsewidths (FWHM) of five individual measurements.

Therefore, the optimum fiber length z_{opt} for compression of the 490 nm pulses should be 94 cm. The compression ratio τ_0/τ is 4.05, showing a compression of the pulses from 800 to about 200 fs.

Fig. 10 shows a plot of the duration of the pulses after the prism compressor as a function of the compressor prism separation; the inset shows the layout of the prism compressor. The pulse duration was determined with the multiple-shot autocorrelator (Inrad 514-A). The optimum compressor baselength is ~100 cm, giving a pulsewidth of ~190 fs (FWHM), which is in good agreement with the theoretical calculation. There is, however, some uncertainty in the measured pulsewidths for the shortest pulses because the 0.5 mm thick BBO crystal in the autocorrelator limits the resolution of the autocorrelator for the shortest pulses. A typical intensity autocorrelation trace of the output from the fiber–prism compressor stage for the optimum compressor baselength is given in Fig. 11. The FWHM is 310 fs, corresponding to a pulse length of ~200 fs (FWHM) for a sech^2 pulse shape. The bandwidth of the pulses was measured with an optical multichannel analyzer (OMA) to be ~2.1 nm, indicating that the shortest pulses are < two times the transform limit for a sech^2 pulse.

At 490 nm, the output from the compressor was amplified in the two-stage dye amplifier to 1.2 mJ, compared to ~1.5 mJ for the longer pulses at this wavelength (only a 20% loss). With the addition of the compressor stage, both the energy and pulse length of the input pulses to the dye amplifiers had greater shot-to-shot variations because of small energy fluctuations in the input to the fiber; however, because of the relatively high saturation levels in the amplifier stages, the energy stability of the amplified, compressed dye pulses was the same as that for the 800 fs pulses (~20% peak-to-peak). The pulse length of the compressed pulses after the amplifier still had the shot-to-shot variation that was present from the compressor stage, with pulsewidths ranging from ~200 to 500 fs; however, there was no tendency for pulse broadening in the dye amplifiers since pulses as short as 200 fs were routinely

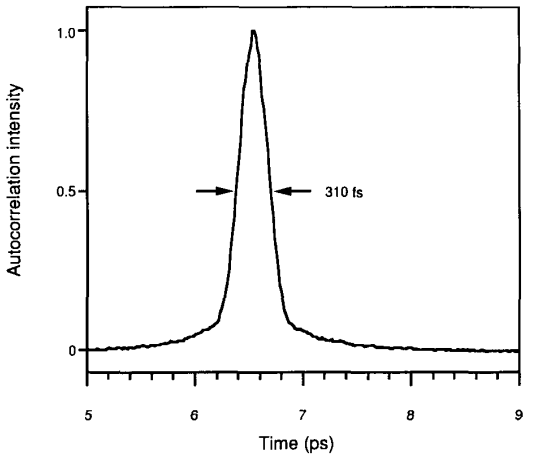

Fig. 11. Autocorrelation trace of the fiber-prism compressor stage output. The data were measured with a multishot background-free autocorrelator. The 310 fs (FWHM) autocorrelation width corresponds to a pulse length of 200 fs, assuming a sech^2 pulse shape.

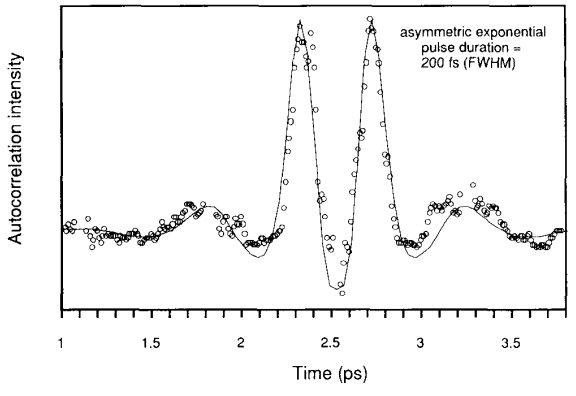

Fig. 12. Autocorrelation trace of the dye amplifier output with the fiber and prism compressor inserted prior to the dye amplifier, measured with a phase-sensitive single-shot autocorrelator [12]. The line indicates a calculated fit to the data assuming an asymmetric exponential pulse with a corresponding pulse width of 200 fs (FWHM).

observed. Fig. 12 shows an autocorrelation trace of an amplified compressed pulse taken with the phase-sensitive single-shot autocorrelator [12]. The fit to the data assuming an asymmetric exponential pulse represents a pulse duration of 200 fs (FWHM).

Since the optimal compressor length changes during tuning, requiring the reoptimization of the timing of the whole amplifier chain, the system was initially designed with the prism compressor after the dye amplifier stages. This design, however, was not viable because the output energy densities from the amplifier were large enough to cause induced absorption in the prisms, resulting in very high losses through the compressor and in damage to the prisms. The damage could be avoided by using beam expanders to enlarge the beam on the prism, but the beam expanders would also result in further losses.

Discussion

Previous millijoule subpicosecond amplifiers have generally relied on a three-dye-cell configuration [6]. For systems utilizing pump pulses longer than the spontaneous emission lifetimes of the dye, three dye cells allowed energy to be sacrificed, from the inclusion of saturable absorbers in the system to suppress ASE, and then recovered in the subsequent dye stages. Other designs using short pump pulses such as from regenerative amplifier systems, however, generally followed the design characteristics of the long pump pulse amplifiers, but demonstrated somewhat higher efficiencies due to lower ASE losses. The two-stage amplifier system presented here was designed specifically for short pump pulses, and it can be used in any case when the input energy to the first stage is sufficient to reach the desired gain saturation level in one dye cell. Assuming that the smallest practical diameter and highest achievable gain at the first cell is 0.1 mm and 10^5, respectively, and using 10 mJ/cm^2 for the output energy density, the minimal input energy is estimated to be 10 pJ, which covers a practical variety of input sources. The use of three amplifier stages would drastically increase the ASE content of the output since, in this case, the system would contain two directly coupled amplifier stages because of the lack of good saturable absorbers. The three-cell design is necessary only when significant throughput losses due to the incorporation of saturable absorbers in the system must be recovered. The high degree of ASE suppression without using saturable absorbers also makes this two-stage system design suitable for other low-gain blue dyes. In addition, by avoiding the use of a saturable absorber, maximum tunability through the two-stage amplifier was maintained.

Amplifier systems designed to operate with red dyes generally incorporate one or more longitudinally pumped amplifier stages to achieve better beam quality; with blue dyes, however, the less favorable σ_e/σ_a ratio (where σ_e is the emission cross section at the amplification wavelength, and σ_a is the absorption cross section at the pump wavelength) and higher excited state absorption generally result in lower performance with longitudinal pumping. This system, therefore, was based only on transversely pumped amplifiers. The design presented here with symmetrical transverse pumping, however, showed little loss of beam spatial quality, which may also be applicable to other dyes.

In summary, the two-stage amplifier design was capable of amplifying subpicosecond pulses to the millijoule level with a very low ASE content, a good beam profile, and no significant pulse broadening. The 800 fs pulses from the dye amplifier had output energies from ~ 1 to 2 mJ throughout a 40 nm tuning range. The 200 fs compressed pulses, obtained by the addition of a fiber and prism compressor, had output energies > 1 mJ, but the system was no longer easily tunable.

ACKNOWLEDGMENT

The authors gratefully acknowledge discussions with C. Jaska, W. Bolt, and J. Tyminski of Coherent, Inc.; Dr. I. Kao of CSK Company, Ltd.; and Dr. J. Weston of Continuum Corporation; and they thank Hammamatsu Inc. for the loan of a streak camera.

REFERENCES

[1] P. M. W. French and J. R. Taylor, "Generation of sub-100-fsec pulses tunable near 497 nm from a colliding-pulse mode-locked ring dye laser," *Opt. Lett.*, vol. 13, pp. 470–472, 1988.

[2] D. K. Negus, B. C. Couillaud, and R. Brady, "Generation of intense tunable femtosecond pulses in the deep blue spectral region," in *Ultrafast Phenomena VI*, T. Yajima, K. Yoshihara, C. B. Harris, and S. Shionoya, Ed. Berlin: Springer-Verlag, 1988, pp. 97–100.

[3] S. Szatmári and F. P. Schäfer, "Subpicosecond, widely tunable distributed feedback dye laser," *Appl. Phys. B*, vol. 46, pp. 305–311, 1988.

[4] A. Migus, A. Antonetti, J. Etchepare, D. Hulin, and A. Orszag, "Femtosecond spectroscopy with high-power tunable optical pulses," *J. Opt. Soc. Amer. B*, vol. 2, pp. 584–594, 1985.

[5] R. W. Schoenlein, J. Y. Bigot, M. T. Portella, and C. V. Shank, "Generation of blue-green 10 fs pulses using an excimer pumped dye amplifier," in *Conf. Lasers Electro-Opt. 1990 Tech. Dig. Ser. Vol. 7*. Washington, DC: Opt. Soc. Amer. 1990, pp. 610–613.

[6] R. L. Fork, C. V. Shank, and R. T. Yen, "Amplification of 70-fs optical pulses to gigawatt powers," *Appl. Phys. Lett.*, vol. 41, pp. 223–225, 1982.

[7] T. Norris, T. Sizer, II, and G. Mourou, "Generation of 85-fs pulses by synchronous pumping of a colliding pulse modelocked dye laser," *J. Opt. Soc. Amer. B*, vol. 2, pp. 613–615, 1985.

[8] M. D. Dawson, W. A. Schroeder, D. P. Norwood, and A. L. Smirl, "Wavelength-tunable synchronous amplification of picosecond dye-laser pulses near 1 μm," *Opt. Lett.*, vol. 14, pp. 364–366, 1989.

[9] T. E. Sharp, Th. Hofmann, C. B. Dane, W. L. Wilson, Jr., F. K. Tittel, P. J. Wisoff, and G. Szabó, "Ultrashort laser pulse amplification in a XeF($C \rightarrow A$) excimer amplifier," *Opt. Lett.*, vol. 15, pp. 1461–1463, 1990.

[10] J. Tyminski, private communication. See also "LBO produces 6 W at 532 nm from mode-locked Nd:YAG," *Laser Focus World*, vol. 26, p. 11, 1990, and "Coherent team gets 6-W SHG from LBO and modelocked YAG," *Lasers & Optronics*, vol. 9, p. 9, 1990.

[11] B. Wu, N. Chen, C. Chen, D. Deng, and Z. Xu, "Highly efficient ultraviolet generation at 355 nm in LiB_3O_5," *Opt. Lett.*, vol. 14, pp. 1080–1081, 1989.

[12] G. Szabó, Z. Bor, and A. Müller, "Phase-sensitive single-pulse autocorrelator for ultrashort laser pulses," *Opt. Lett.*, vol. 13, pp. 746–748, 1988.

[13] W. J. Tomlinson, R. H. Stolen, and C. V. Shank, "Compression of optical pulses chirped by self-phase modulation in fibers," *J. Opt. Soc. Amer. B*, vol. 1, pp. 139–149, 1984.

[14] G. Szabó, T. E. Sharp, F. K. Tittel, and P. J. Wisoff, "Dispersion measurements of single-mode fibers in the blue-green spectral region by an interferometric method," submitted to *Appl. Opt.*

Tracy E. Sharp (S'89) was born in Tampa, FL, in 1966. She received the B.S. and M.S. degrees in electrical engineering from Rice University, Houston, TX, in 1988 and 1990, respectively.

She is presently working towards the Ph.D. degree in electrical engineering at Rice University.

Ms. Sharp is a member of Tau Beta Pi, Eta Kappa Nu, the IEEE Lasers and Electro-Optics Society, and the Optical Society of America.

C. Brent Dane . for a photograph and biography, see p. 262 of the February 1991 issue of this JOURNAL.

Duane Barber, photograph and biography not available at the time of publication.

Frank K. Tittel (SM'72–F'86), for a photograph and biography, see p. 100 of the January 1991 issue of this JOURNAL.

Peter J. Wisoff (M'86), for a photograph and biography, see p. 100 of the January 1991 issue of this JOURNAL.

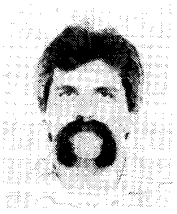

Gabor Szabó was born in Hungary in 1954. He received the M.S. and Ph.D. degrees in physics from JATE University, Szeged, Hungary, in 1978 and 1981, respectively.

From 1984 to the present, he has been at JATE University where he is an Associate Professor in the Department of Optics and Quantum Electronics. In addition he has been a Visiting Scientist at both the Max-Planck Institute, Göttingen, Germany, and Rice University, Houston, TX.

Dr. Szabó is a member of the Hungarian Physical Society.